Supporting Information

Pt atoms on doped carbon nanosheets with ultrahigh N content as a superior bifunctional catalyst for hydrogen evolution/oxidation

Zhen Zhang [a, b], Cheng Jiang [b], Ping Li [c], Qi Feng [b], Zhiliang Zhao [b], Keguang Yao [b], Jiantao Fan [b], Hui Li [b *], Haijiang Wang [d]

a School of Materials Science and Engineering, Harbin Institute of Technology, Harbin 150001, China

b Department of Materials Science and Engineering, Shenzhen Key Laboratory of Hydrogen Energy, Southern University of Science and Technology, Shenzhen 518055, Guangdong, China

c Center for Spintronics and Quantum Systems, State Key Laboratory for Mechanical Behavior of Materials, School of Materials Science and Engineering, Xi'an Jiaotong University, Xi'an, Shaanxi, 710049, China

d Department of Mechanical and Energy Engineering, Southern University of Science and Technology, Shenzhen, 518055, China

*Corresponding author:

E-mail address: hui.li@sustech.edu.cn

Keywords: hydrogen evolution, hydrogen oxidation, single atom catalyst, electrolyzer, fuel cell

Experimental Section

1. Three-electrode electrochemical measurements

For HER, the Tafel slopes were fitted based on the Tafel equation:

$$\eta = a + b \log(j) \qquad (1)$$

where η (mV) indicates the applied overpotential, j (mA cm^{-2}) denotes the current density, and b (mV dec^{-1}) is the Tafel slope. Electrochemical double-layer capacitance (C_{dl}) in 0.5 M H_2SO_4 was used to determine the electrochemical active surface area (ECSA) of the prepared catalysts. The C_{dl} was detected from CV curves measured in the potential range of 0.15–0.25 V. C_{dl} was calculated according equation (2):

$$C_{dl} = \Delta j/2v \qquad (2)$$

where $\Delta j = |j_a| - |j_c|$ and v is the scan rate. The values of j_a and j_c were taken at a potential of 0.2 V.

For HOR, the measured overall current (j) is a combination of the kinetic (j_k) and diffusional (j_d) components. Based on previous reports, the current is proportional to the square root of the rotation speed, according to the Koutecky-Levich equation:

$$1/j = 1/j_k + 1/j_d \qquad (3)$$

$$j_d = 0.62nFD^{2/3}v^{-1/6}c_0\omega^{1/2} \qquad (4)$$

where j is the detectable current density, j_k is the kinetic current in the absence of mass transfer limitations, and j_d is the diffusion current density. Using equation (4), j_d can be calculated, where n is the number of electrons transferred, F is the Faraday constant, D is the diffusion coefficient of the reactant, v is the viscosity of the electrolyte, c_0 is the solubility of H_2 in the electrolyte, and ω is the rotating speed. The inverse of the current density at a fixed potential can be linearly fitted with respect to $\omega^{-1/2}$, and the intercept of the extrapolated line indicates the inverse of the pure kinetic current density.

2. Computational details

DFT calculations were performed using the Vienna Ab initio Simulation Package (VASP) and the Perdew-Burke-Ernzerhof (PBE) exchange-correlation functional correction.[1] The hydrogen binding energy (ΔE_{H*}) value was obtained using the

following equation:[2]

$$\Delta E_{H^*} = E_{H^*@surface} - E_{surface} - 1/2E_{H2} \quad (5)$$

where $E_{H^*@surface}$ and $E_{surface}$ are the energies of the H absorbed systems and the clean given surface, respectively, and E_{H2} is the energy of molecular H_2 in the gas phase. Atomic relaxation was conducted until the total energy variation was less than 10^{-6} eV and all forces on each atom were less than 0.01 eV $Å^{-1}$. In addition, the electron wave functions were expanded, with a plane wave cutoff of 400 eV.

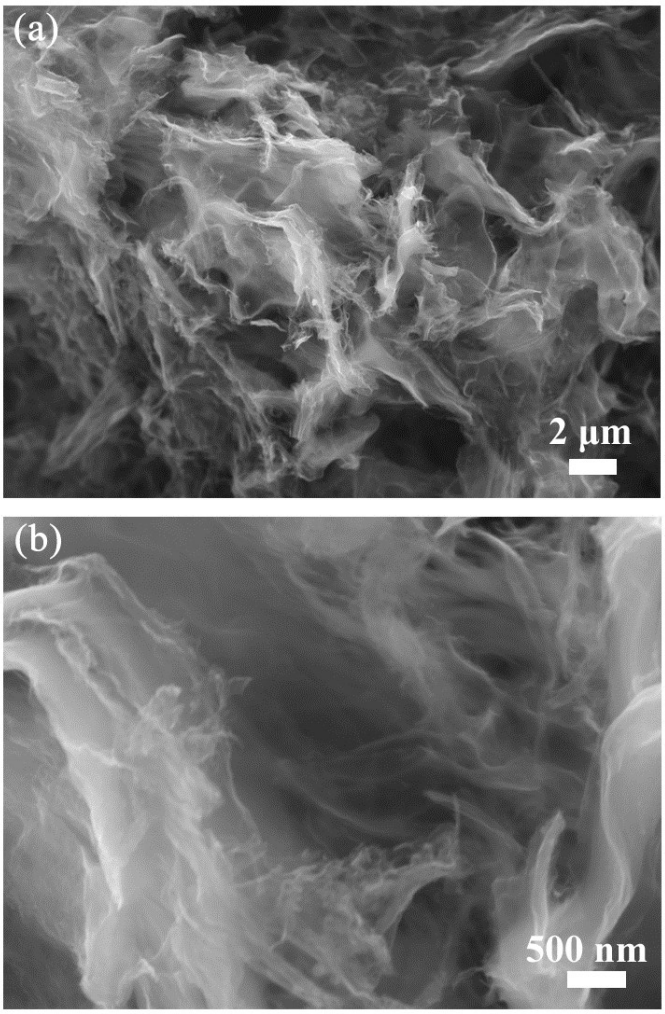

Figure S1. SEM images of pure NCS support.

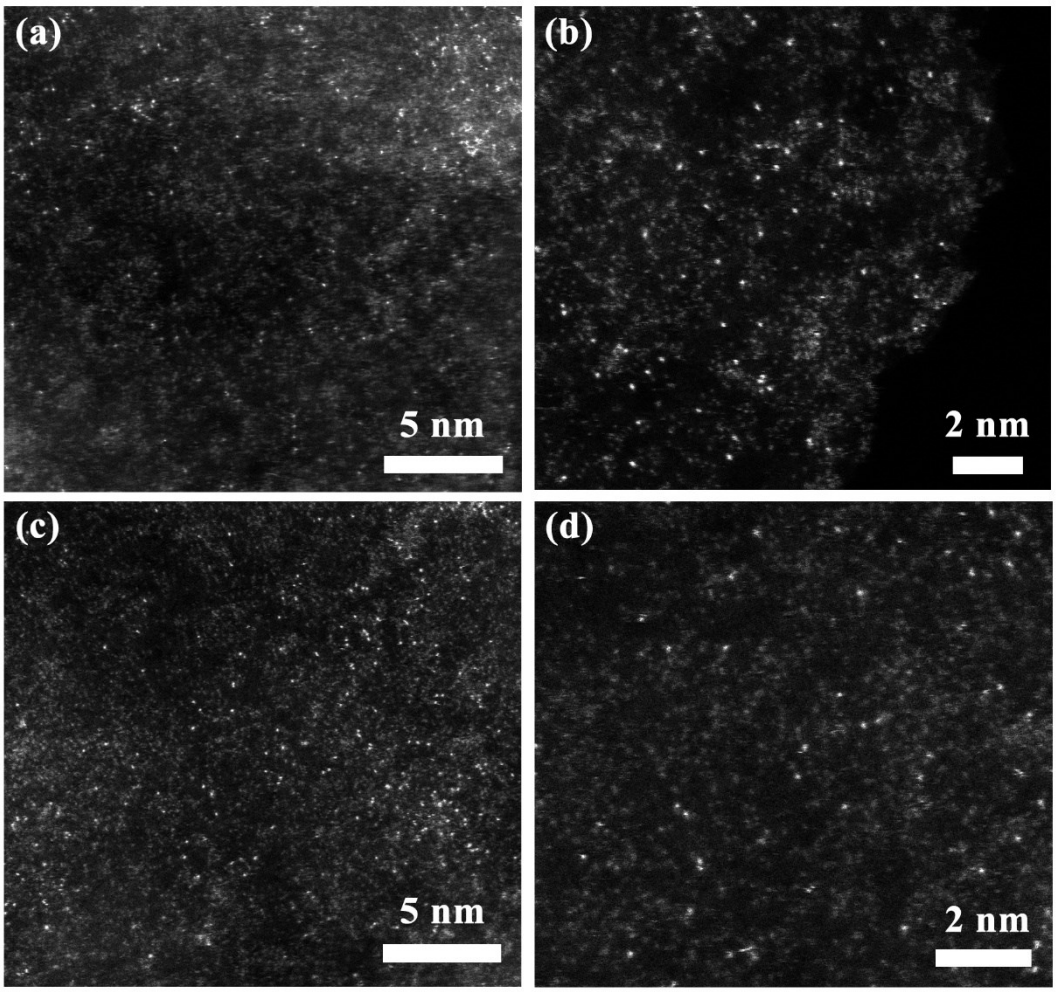

Figure S2. HAADF-STEM images of Pt/NCS detected from different sections.

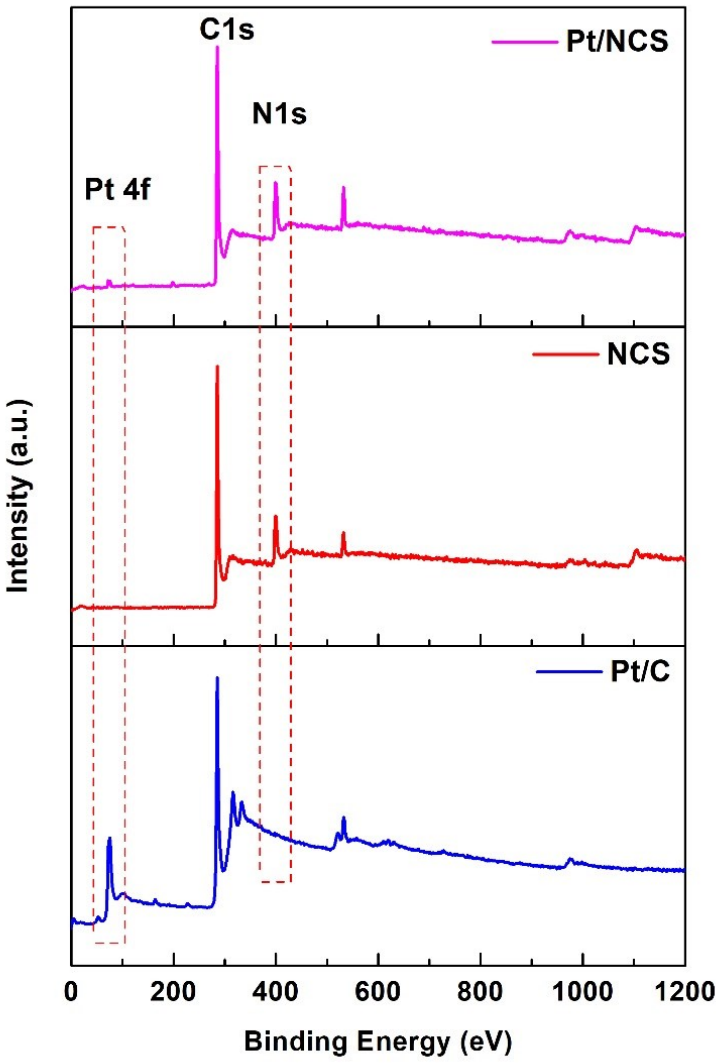

Figure S3. XPS survey for commercial Pt/C, NCS support, and Pt/NCS.

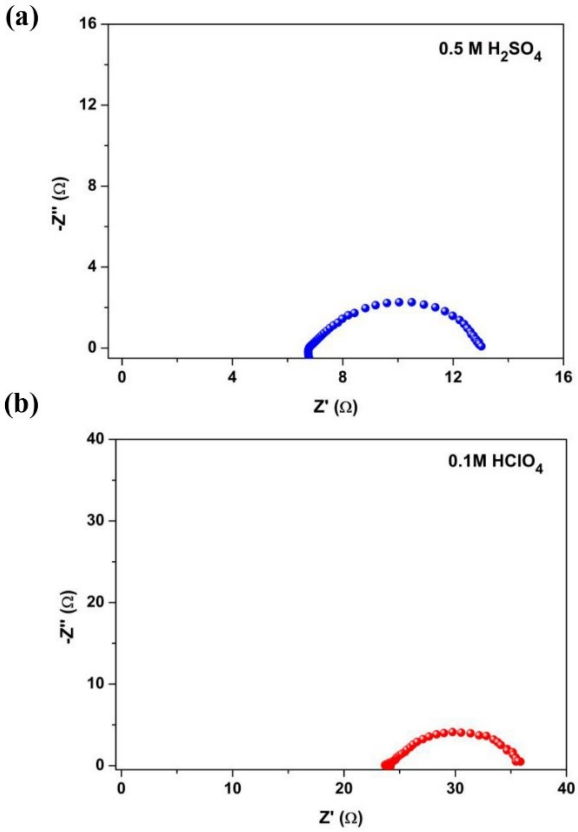

Figure S4. Nyquist plots of Pt/NCS at –0.05V *vs*. RHE in (a) 0.5 M H_2SO_4 and (b) 0.1 M $HClO_4$ media.

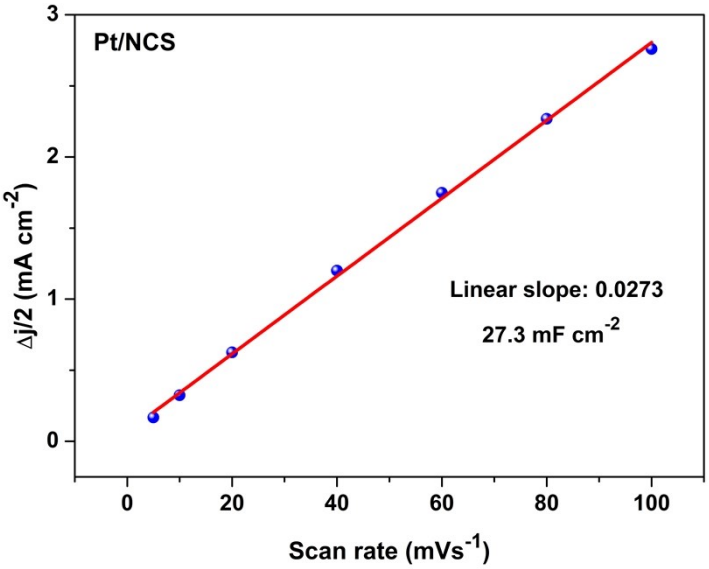

Figure S5. Linear fitting for the double-layer capacitance (C_{dl}) value of Pt/NCS.

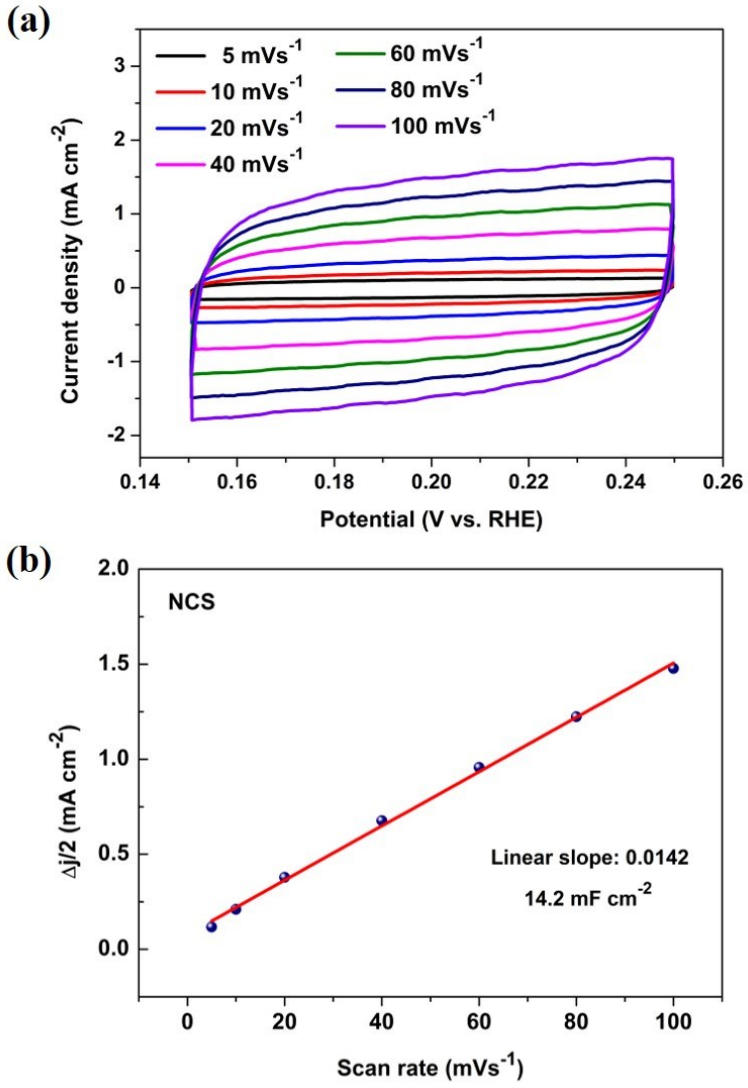

Figure S6. (a) CV curves at various scan rates and (b) linear fitting for the double-layer capacitance values of pure NCS.

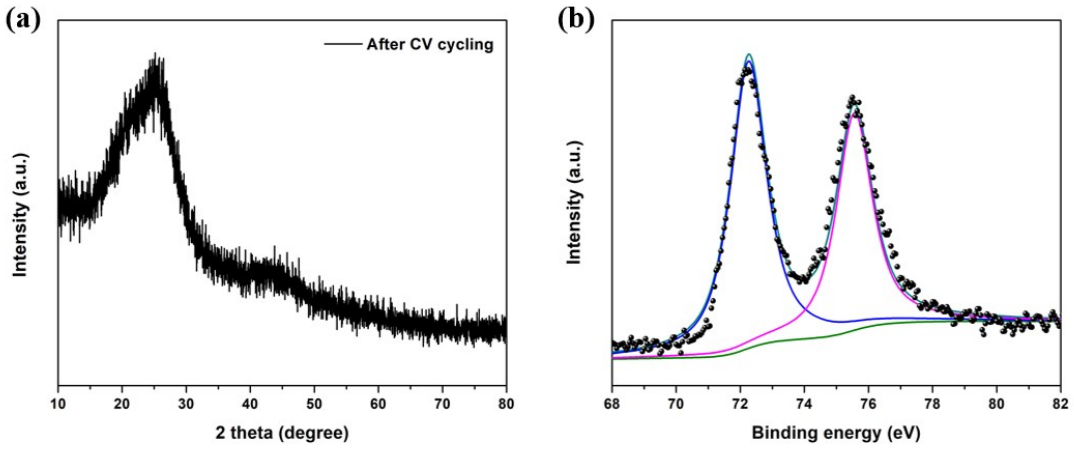

Figure S7. (a) XRD and (b) high-resolution Pt 4f patterns of Pt/NCS after 2000 CV cycles testing.

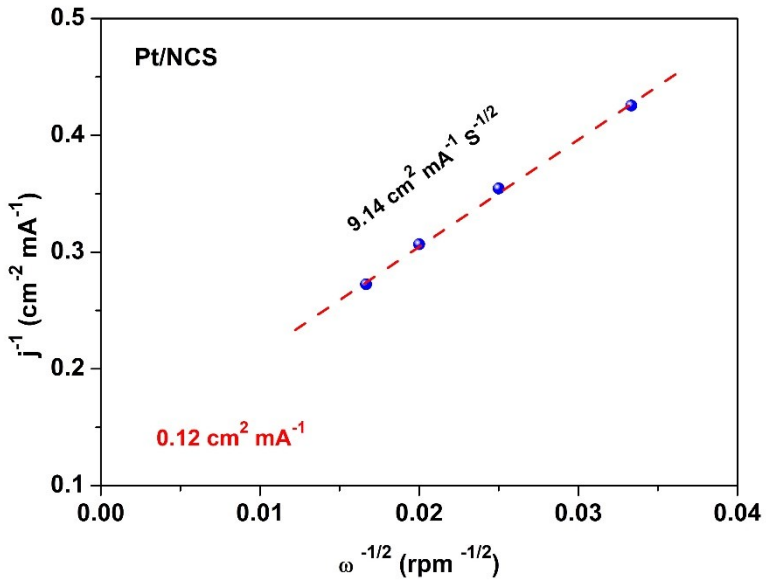

Figure S8. Koutecky-Levich plot for the HOR at 0.05 V of Pt/NCS.

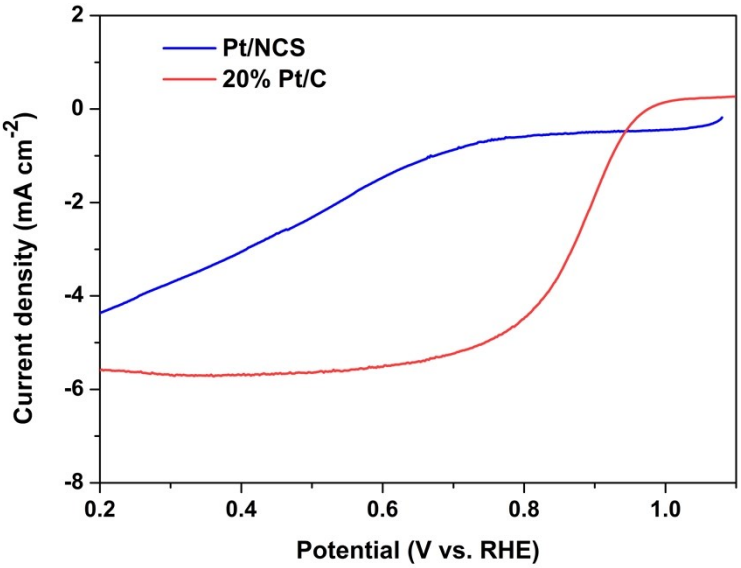

Figure S9. Polarization curves of the ORR for Pt/NCS and commercial 20% Pt/C with O_2-saturated 0.1 M $HClO_4$.

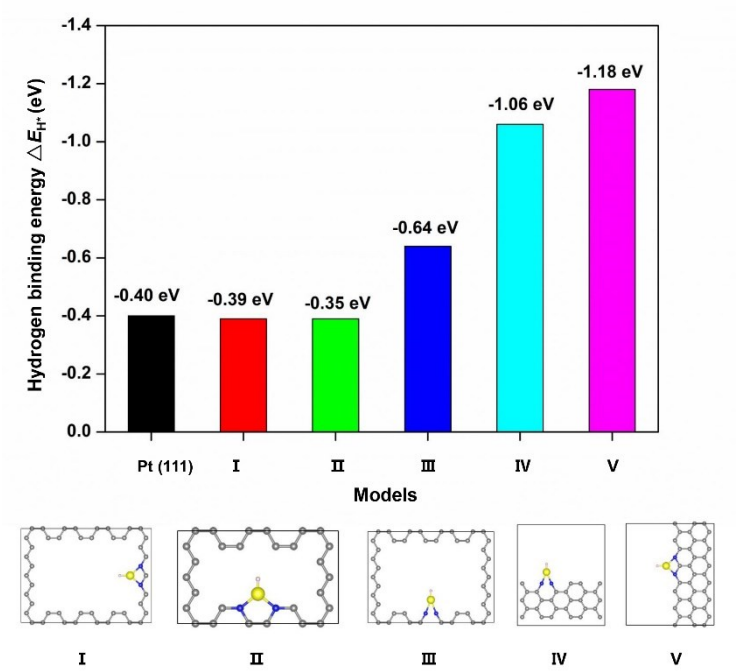

Figure S10. The hydrogen binding energy ΔE_{H^*} diagram for various Pt/NCS configurations, as well as Pt (111) for comparison. The DFT optimized models are shown on the bottom. The C, N, Pt and H atoms are represented as gray, blue, yellow and white spheres, respectively.

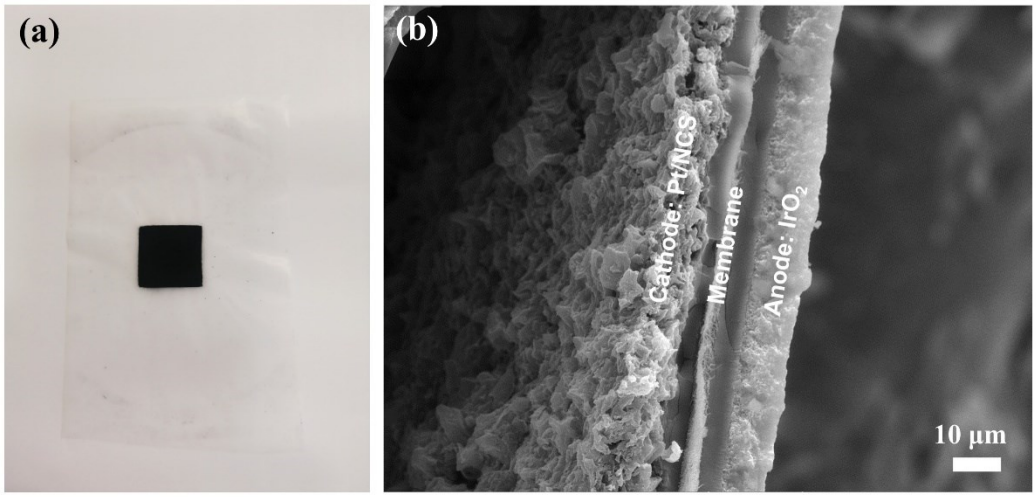

Figure S11. (a) Photo of CCM and (b) SEM image of the cross-section using Pt/NCS and IrO_2 as cathode and anode, respectively.

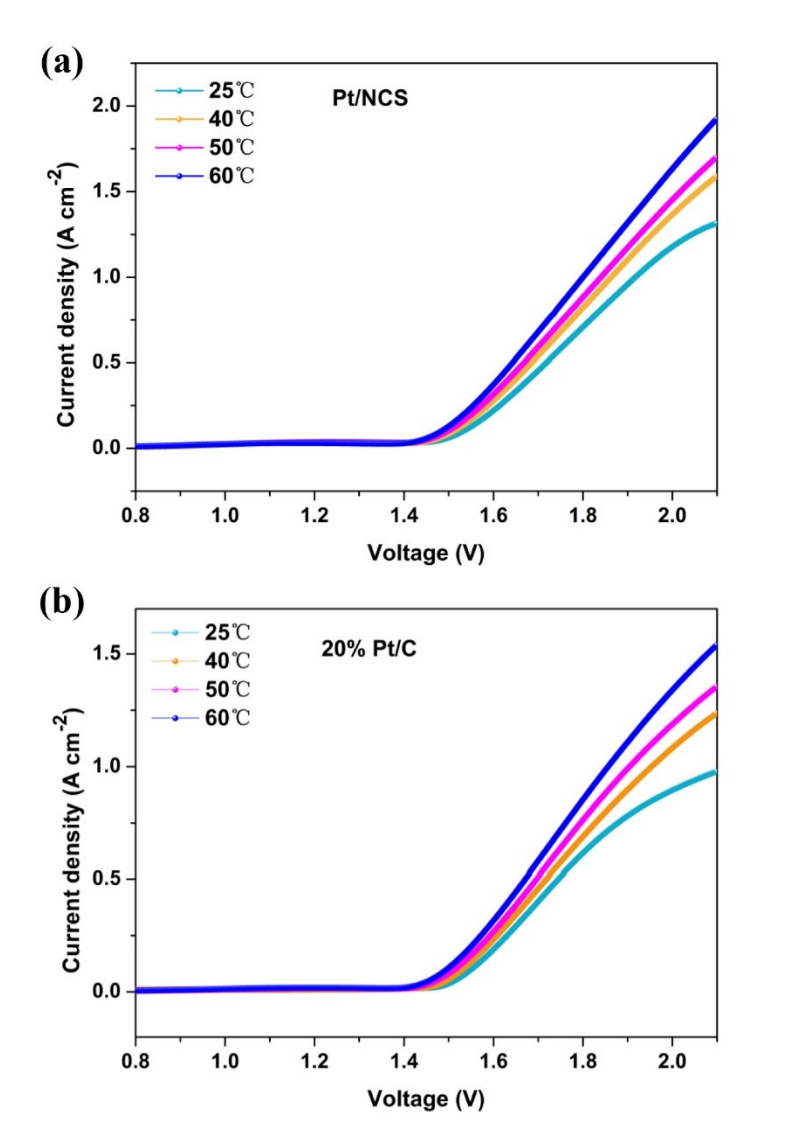

Figure S12. Polarization curves obtained with homemade PEM electrolyzer device using (a) Pt/NCS and (b) 20% Pt/C as cathode at various temperatures.

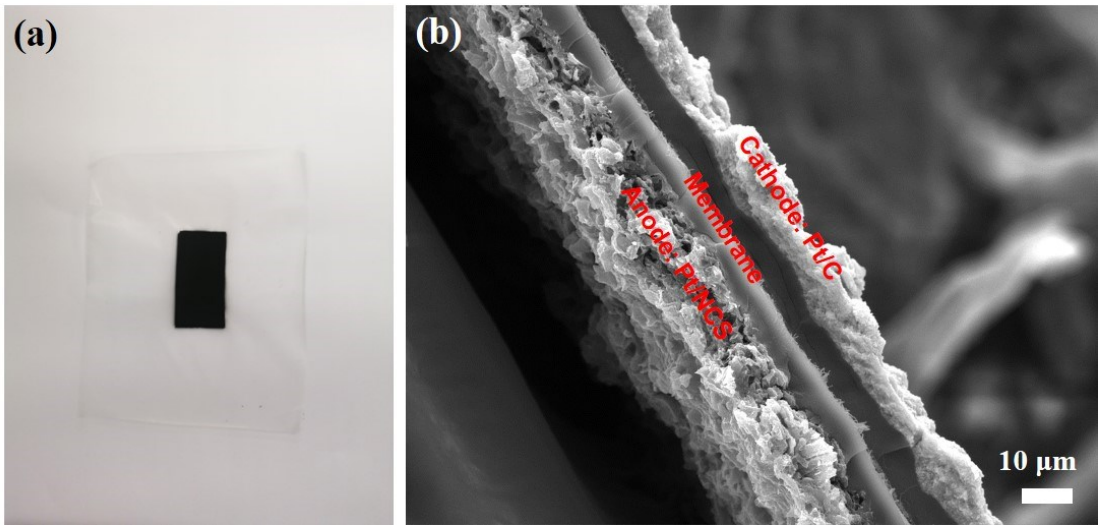

Figure S13. (a) Photo of CCM and (b) SEM image of the cross-section using Pt/NCS and commercial 47% Pt/C as anode and cathode, respectively.

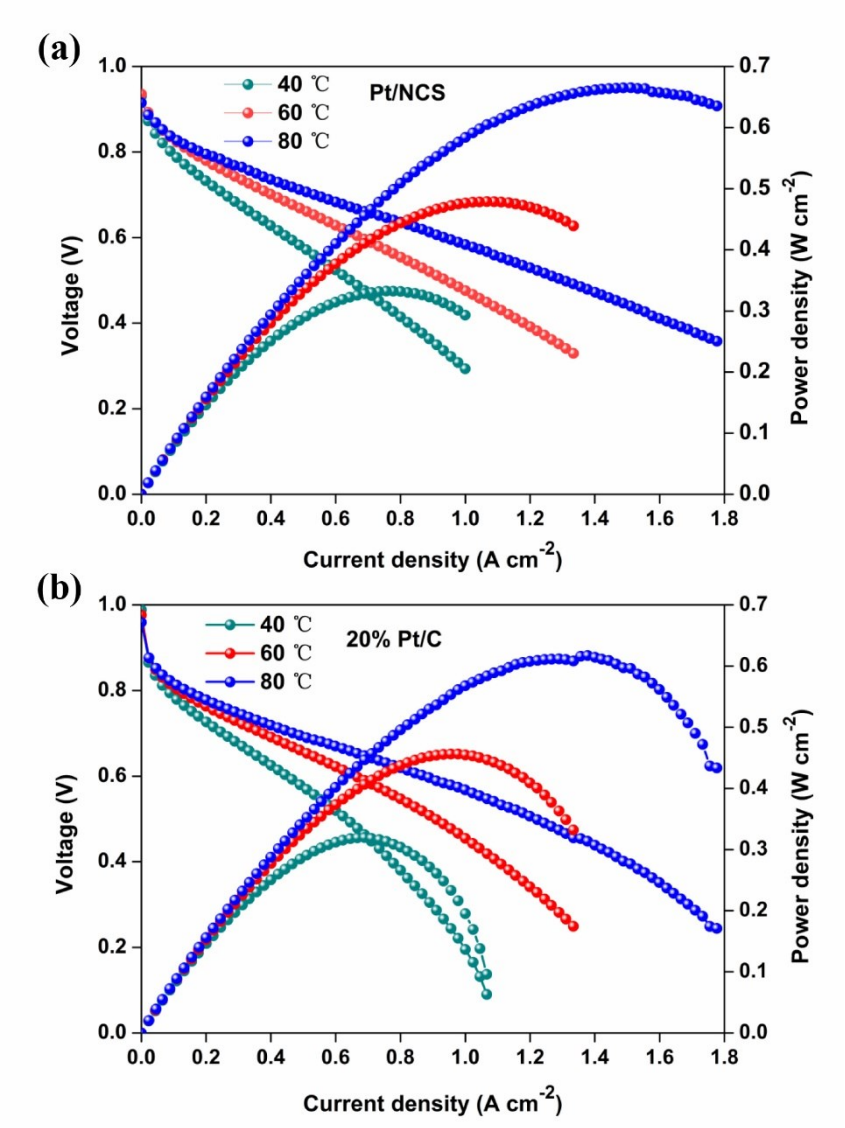

Figure S14. Polarization curves obtained with homemade PEM fuel cell device using (a) Pt/NCS and (b) 20% Pt/C as anode at various temperatures.

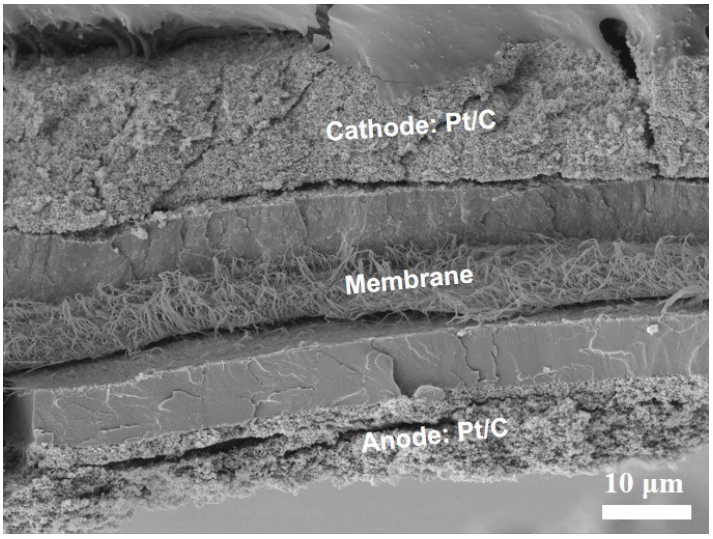

Figure S15. SEM image of the cross-section using commercial 20% Pt/C and 47% Pt/C as anode and cathode, respectively.

Table S1. EXAFS fitting parameters at the Pt L_3-edge for Pt/NCS.

Sample	Shell	CN	R(Å)	σ^2	ΔE_0	R factor
Pt/NCS	Pt-N	2.0±0.4	1.89±0.03	0.0045	8.7±1.9	0.0081

Note:

CN: coordination number
R: distance between absorber and backscatter atoms
σ^2: Debye–Waller factors
ΔE_0: inner potential correction
R factor: goodness of the fitting.

Table S2. HER performance for recently reported atomically dispersed Pt-based catalysts in acidic medium.

Sample	Overpotential at 10 mA cm^{-2} (mV)	Tafel slope (mV dec^{-1})	Pt loading (mg cm^{-2})	Ref.
Pt/NCS	18.1 @ 10 89.1 @ 100	30	0.00408	This work
ALD Pt on NGNs with 50 cycles	45	NA	0.00161	[3]
Pt_1/NPC	25	28	0.0038	[4]
400-SWNT/Pt	27	38	~0.01942	[5]
Pt/f-MWCNTs	43.9	30	0.000914	[6]
Pt_1/hNCNC-2.92	15	24	0.00287	[7]
Pt_1/OLC	38	36	0.001377	[8]
Pt@PCM	105@10 142@20	65.3	N.A.	[9]
Pt_1/MC	25	26	0.010	[10]
AC Pt-NG/C	35.2	27	0.00566	[11]
1-Pt-NG/C	47.2	31	0.00283	[11]
Pt SAs/DG	23	25	0.021	[12]
Pt/NMC-LT	17	26.3	0.010	[13]
Pt_1/NMC	29	26	0.010	[14]
Pt-SA/α-MoO_X	19	123	0.00168	[15]
Pt@MoS_2/NiS_2	34	40	0.01026	[16]
Pt/NiS@Al_2O_3	34	35	0.01596	[17]
Pt/np-$Co_{0.85}Se$	58	26	NA	[18]
Pt-GDY2	~70	46.6	0.00465	[19]

Mo_2TiC_2TX-Pt_{SA}	30	30	0.012	[20]
Pt_1@Fe-N-C	60	42	0.0084	[21]
Pd/Cu-Pt nanorings	22.8	25	0.0408	[22]

References

1. J. P. Perdew, K. Burke and M. Ernzerhof, *Physical Review Letters*, 1996, **77**, 3865-3868.
2. J. K. Nørskov, T. Bligaard, A. Logadottir, J. R. Kitchin, J. G. Chen, S. Pandelov and U. Stimming, *Journal of The Electrochemical Society*, 2005, **152**, J23.
3. N. Cheng, S. Stambula, D. Wang, M. N. Banis, J. Liu, A. Riese, B. Xiao, R. Li, T. K. Sham, L. M. Liu, G. A. Botton and X. Sun, *Nat Commun*, 2016, **7**, 13638.
4. T. Li, J. Liu, Y. Song and F. Wang, *ACS Catalysis*, 2018, **8**, 8450-8458.
5. M. Tavakkoli, N. Holmberg, R. Kronberg, H. Jiang, J. Sainio, E. I. Kauppinen, T. Kallio and K. Laasonen, *ACS Catalysis*, 2017, **7**, 3121-3130.
6. J. Ji, Y. Zhang, L. Tang, C. Liu, X. Gao, M. Sun, J. Zheng, M. Ling, C. Liang and Z. Lin, *Nano Energy*, 2019, **63**, 103849.
7. Z. Zhang, Y. Chen, L. Zhou, C. Chen, Z. Han, B. Zhang, Q. Wu, L. Yang, L. Du, Y. Bu, P. Wang, X. Wang, H. Yang and Z. Hu, *Nat Commun*, 2019, **10**, 1657.
8. D. Liu, X. Li, S. Chen, H. Yan, C. Wang, C. Wu, Y. A. Haleem, S. Duan, J. Lu, B. Ge, P. M. Ajayan, Y. Luo, J. Jiang and L. Song, *Nature Energy*, 2019, **4**, 512-518.
9. H. Zhang, P. An, W. Zhou, B. Y. Guan, P. Zhang, J. Dong and X. W. Lou, *Science Advances*, 2018, **4**, eaao6657.
10. H. Wei, K. Huang, D. Wang, R. Zhang, B. Ge, J. Ma, B. Wen, S. Zhang, Q. Li, M. Lei, C. Zhang, J. Irawan, L. M. Liu and H. Wu, *Nat Commun*, 2017, **8**, 1490.
11. M. Sun, J. Ji, M. Hu, M. Weng, Y. Zhang, H. Yu, J. Tang, J. Zheng, Z. Jiang, F. Pan, C. Liang and Z. Lin, *ACS Catalysis*, 2019, **9**, 8213-8223.
12. Y. Qu, B. Chen, Z. Li, X. Duan, L. Wang, Y. Lin, T. Yuan, F. Zhou, Y. Hu, Z. Yang, C. Zhao, J. Wang, C. Zhao, Y. Hu, G. Wu, Q. Zhang, Q. Xu, B. Liu, P. Gao, R. You, W. Huang, L. Zheng, L. Gu, Y. Wu and Y. Li, *J Am Chem Soc*, 2019, **141**, 4505-4509.
13. K. Huang, R. Wang, H. Wu, H. Wang, X. He, H. Wei, S. Wang, R. Zhang, M. Lei, W. Guo, B. Ge and H. Wu, *Journal of Materials Chemistry A*, 2019, **7**, 25779-25784.
14. H. Wei, H. Wu, K. Huang, B. Ge, J. Ma, J. Lang, D. Zu, M. Lei, Y. Yao, W. Guo and H. Wu, *Chem Sci*, 2019, **10**, 2830-2836.
15. J. Xu, C. Zhang, H. Liu, J. Sun, R. Xie, Y. Qiu, F. Lü, Y. Liu, L. Zhuo, X. Liu and J. Luo, *Nano Energy*, 2020, **70**, 104529.
16. Y. Guan, Y. Feng, J. Wan, X. Yang, L. Fang, X. Gu, R. Liu, Z. Huang, J. Li, J. Luo, C. Li and Y. Wang, *Small*, 2018, **14**, e1800697.
17. Y. Feng, Y. Guan, H. Zhang, Z. Huang, J. Li, Z. Jiang, X. Gu and Y. Wang, *Journal of Materials Chemistry A*, 2018, **6**, 11783-11789.
18. K. Jiang, B. Liu, M. Luo, S. Ning, M. Peng, Y. Zhao, Y. R. Lu, T. S. Chan, F. M. F. de Groot and Y. Tan, *Nat Commun*, 2019, **10**, 1743.
19. X. P. Yin, H. J. Wang, S. F. Tang, X. L. Lu, M. Shu, R. Si and T. B. Lu, *Angew Chem Int Ed Engl*, 2018, **57**, 9382-9386.
20. J. Zhang, Y. Zhao, X. Guo, C. Chen, C.-L. Dong, R.-S. Liu, C.-P. Han, Y. Li, Y. Gogotsi and G. Wang, *Nature Catalysis*, 2018, **1**, 985-992.
21. X. Zeng, J. Shui, X. Liu, Q. Liu, Y. Li, J. Shang, L. Zheng and R. Yu, *Advanced Energy Materials*, 2018, **8**, 1701345.
22. T. Chao, X. Luo, W. Chen, B. Jiang, J. Ge, Y. Lin, G. Wu, X. Wang, Y. Hu, Z. Zhuang, Y.

Wu, X. Hong and Y. Li, *Angew Chem Int Ed Engl*, 2017, **56**, 16047-16051.